Orientational Order of Locally Parallel Chain Segments in Glassy Polycarbonate from $^{13}C-^{13}C$ Dipolar Couplings

Christopher A. Klug,[†] Wenlian Zhu,[‡] Kenzabu Tasaki,[§] and Jacob Schaefer*

Department of Chemistry, Washington University, St. Louis, Missouri 63130

Received July 30, 1996; Revised Manuscript Received December 3, 1996[⊗]

ABSTRACT: Interchain $^{13}C-^{13}C$ distances between ^{13}C labels and between ^{13}C labels and natural-abundance ^{13}C have been determined using dipolar restoration at the magic angle (DRAMA) with XY8 phase alternation and controlled simple excitation for dephasing rotational amplitudes (CEDRA) for two samples: (i) [carbonyl-^{13}C]polycarbonate and (ii) a homogeneous blend of 95% [carbonyl-^{13}C]polycarbonate-d_{14} and 5% [methyl-^{13}C]polycarbonate. DRAMA is suitable for dipolar-coupled $^{13}C-^{13}C$ pairs having the same isotropic chemical shift, whereas CEDRA is used for pairs with dissimilar isotropic shifts. Pairs with dissimilar shifts were also examined using selective π pulses and a homonuclear version of rotational-echo double resonance called DANTE-Selective REDOR (DSR). The combination of results from DRAMA, CEDRA, and DSR experiments shows that the glass consists on average of densely packed chains. This result is interpreted in terms of the orientational order of locally parallel chain segments (bundles). The bundles are structurally irregular and are characterized by a distribution of interchain spacings, which is consistent with the homonuclear NMR results from this work and with the results of previous heteronuclear distance measurements.

A number of solid-state NMR experiments capable of measuring heteronuclear and homonuclear intermolecular distances have been developed recently.[1−4] The results of such experiments applied to polymers help to define local chain-packing and can be used as starting coordinates for molecular dynamics simulations.[5,6] In previous work, we reported an average intermolecular distance between carbonyl carbons and nearest-neighbor methyl deuterons of 3.8 Å in homogeneous blends of ^{13}C-labeled polycarbonate and ^{2}H-labeled polycarbonate.[7] In addition, we determined nearest-neighbor interchain ring-carbon to ring-deuterium and ring-carbon to methyl-deuterium distances of 2.6 and 3.2 Å, respectively.[8] These distances were determined by $^{13}C-^{2}H$ rotational-echo double resonance (REDOR).[1,7] The short ring−ring distance indicates that the phenyl groups are tightly packed, consistent with the observation that cooperative intermolecular motion is required for ring flips.[9,10]

In this paper, we describe the results of homonuclear dephasing experiments to measure $^{13}C-^{13}C$ distances in pure [carbonyl-^{13}C]polycarbonate and in a homogeneous blend of [carbonyl-^{13}C]polycarbonate-d_{14} and [methyl-^{13}C]polycarbonate. The results of these measurements also suggest tight chain packing, with carbon−carbon distances comparable to those observed by X-ray crystallography for a low-molecular weight crystalline analogue of polycarbonate.[11,12] On the basis of the constraints established by NMR, we propose a model for the packing in polycarbonate of locally parallel chain segments, which we refer to as "bundles". This bundle model accommodates local orientational order and global orientational disorder, as well as structural and conformational heterogeneity.

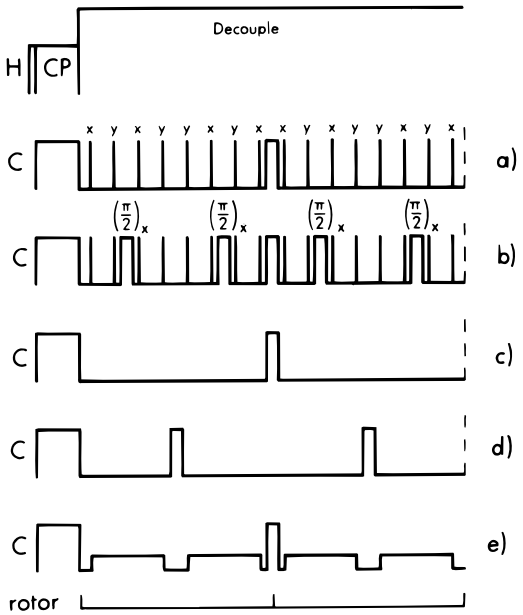

Figure 1. Pulse sequences for a $^{1}H-^{13}C$ matched spin-lock, cross-polarization transfer followed by (a) a compensated DRAMA full echo, (b) a compensated DRAMA dephased echo, (c) a rotor-synchronized Hahn echo, (d) a CEDRA dephased echo, and (e) a DANTE-selected homonuclear REDOR dephased echo. Phase alternation of the refocusing Hahn π pulse after odd-numbered rotor cycles, and that of the eight equally spaced π pulses during each rotor period of the compensated DRAMA sequences, follow the XY8 scheme. All dephasing $\pi/2$ pulses have the same phase. The DANTE-selective π pulse consists of ten 9-μs weak pulses separated by 30 μs. The illustration is for two rotor cycles.

Experiments

DRAMA. Dipolar restoration at the magic angle (DRAMA) uses rotor-synchronized 90° pulses to dephase the magnetization of isolated homonuclear pairs of dipolar-coupled spin-$^1/_2$ nuclei.[3,13] For the DRAMA experiments described here, a rotor-synchronized echo was produced on even-numbered rotor cycles by a refocusing π pulse following the completion of odd-numbered cycles (Figure 1a). These π pulses were phase alternated following the XY8 scheme[14] (xyxyyxyx) which therefore required 16 rotor cycles to complete. The phase of

[†] Present address: Department of Chemical Engineering, Stanford University, Stanford, CA 94305.

[‡] Present address: Howard Hughes Medical Institute, University of Maryland Baltimore County, Baltimore, MD 21228.

[§] Present address: Mitsubishi Chemical America, Inc., San Jose, CA 95143.

[⊗] Abstract published in *Advance ACS Abstracts,* February 1, 1997.

S0024-9297(96)01144-8 CCC: $14.00

the leading pulse of the XY8 sequence was determined by the ^{13}C quadrature routing. Frequency offsets due to variations in chemical shift tensors were refocused using eight equally spaced π pulses per rotor cycle (Figure 1a).[15] These pulses were placed at $^1/_{16}$, $^3/_{16}$, $^5/_{16}$, ... of the rotor period (T_r). Phase accumulation at the spinning frequency and twice the spinning frequency from chemical-shift interactions for transverse magnetization arising from individual crystallites in an isotropic powder tend to cancel under the four sign reversals created in each half rotor cycle by the eight π pulses.[15] The phases of these π pulses were also alternated according to the XY8 scheme. The DRAMA full echo which formed at the completion of even numbers of rotor cycles using the sequence of Figure 1a is S_0. Two 90° pulses per rotor period were placed at $^1/_4$ T_r and $^3/_4$ T_r for maximum DRAMA dephasing. These pulses all had the same phase which was determined by the ^{13}C quadrature routing. The DRAMA-dephased echo which formed at the completion of even numbers of rotor cycles using the sequence of Figure 1b is S.

DRAMA experiments were performed using two channels of a four-channel spectrometer built around an 89-mm, vertical-bore superconducting solenoid operating at 7.05 T. The single, 9-mm diameter, radio-frequency coil was connected by a low-loss transmission line to a $^1H-^{13}C-^2H$ tuning circuit.[7] Samples were spun in zirconia rotors (with 350-mg capacity) at 4167 Hz. Spinning stability to within ±2 Hz was achieved with active control. Power for the radio-frequency pulses was supplied by 1-kW Kalmus LP-1000 and ENI LPI-10H transmitters for ^1H and ^{13}C channels, respectively. The ^{13}C radio-frequency field amplitude was 67 kHz for the matched cross-polarization transfer and DRAMA evolution; the ^1H decoupling field was 100 kHz. The spectrometer was controlled by a four-channel Chemagnetics CMX-300 console. The chemical shift of the carbonyl-carbon peak of polycarbonate is 150 parts per million downfield from tetramethylsilane as an external reference.

CEDRA. Simple excitation for the dephasing of rotational amplitudes (SEDRA) involves the observation of rotational echoes with (S) and without (S_0) rotor-synchronized dephasing.[2] For an isolated $^{13}C-^{13}C$ pair having a significant isotropic shift separation, one π pulse every two rotor periods (Figure 1c) produces refocusing while one π pulse per rotor period (Figure 1d) produces dephasing. The phases of the π pulses followed the XY8 scheme.[14] Therefore, a full echo (S_0) had complete XY8 phase compensation after multiples of 16 rotor cycles, whereas the dephased echo (S) was obtained with full compensation in multiples of 8 rotor cycles. Full echoes were also observed after multiples of 8 rotor cycles using refocusing π pulses at multiples of $2T_r$ and $6T_r$ with simple XY phase alternation. The intensities of these echoes were indistinguishable from those with XY8 phase compensation for comparable evolution times.

For the SEDRA experiments described here, refocusing was optimized by satisfying the CEDRA[16] isotropic chemical-shift separation condition, $\Delta\nu_{iso} = (2n + 1)\nu_r/2$, $n = 1$. The quality of the refocusing (phase and amplitude) for the relatively broad polycarbonate lines was not affected by mismatches of the order of ±100 Hz. CEDRA ^{13}C NMR spectra were obtained at room temperature at 15.1 MHz using a 12-in. resistive magnet and a home-built spectrometer, details of which have been described previously.[17] The single, 11-mm diameter, radio-frequency coil was connected by a low-loss transmission line to a double-resonance tuning circuit. A 1-kW ENI LPI-10H amplifier was used for the ^1H channel, and an ENI A-300 amplifier, for the ^{13}C channel. Cross-polarization transfers were performed at 50 kHz, carbon π pulses were at 50 kHz, and proton dipolar decoupling was at 100 kHz. Rotors with 600-mg sample capacities were made from plastic (Kel-F) and supported at both ends by air-pumped journal bearings. In these experiments, a 350-mg sample was positioned in the center of the rotor by Kel-F spacers.

DSR. Dante-selected homonuclear REDOR (DSR) experiments were performed at 15.1 MHz. A selective π pulse was produced by ten 9-μs pulses with 30-μs spacings. The radio-frequency field amplitude was 5.6 kHz. Each selective π pulse required 360 μs to complete so that a REDOR pair of pulses took approximately $^7/_8$ of the rotor period with 1222-Hz spinning. This spinning speed satisfies the CEDRA $n = 1$ condition. An echo with DSR dephasing was observed using the pulse sequence of Figure 1e. The nonselective π pulse at the completion of odd rotor cycles refocuses isotropic chemical shifts but has no effect on $^{13}C-^{13}C$ dipolar coupling. Phases of these pulses followed the XY8 scheme. The selective π pulses were centered at $T_r/4$ and $3T_r/4$. A full echo was observed by omitting the selective π pulses (Figure 1c) and had full XY8 phase compensation after multiples of 16 rotor cycles.

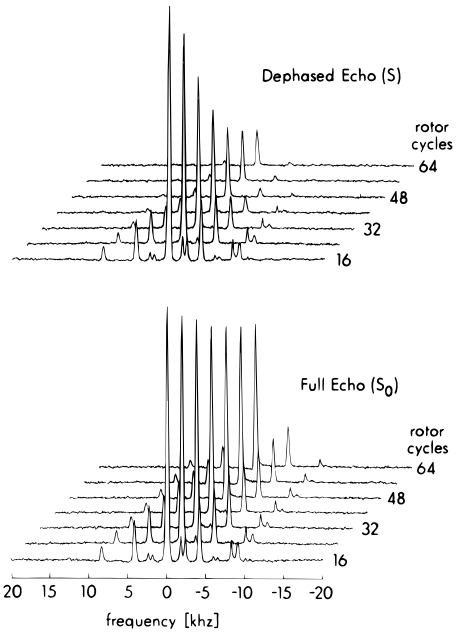

Figure 2. DRAMA dephased-echo (S) and full-echo (S_0) 75-MHz ^{13}C NMR spectra of [carbonyl-^{13}C]polycarbonate as a function of the number of rotor cycles of dephasing with magic-angle spinning at 4167 Hz.

Results

The Hahn-echo ^{13}C NMR spectrum of [carbonyl-^{13}C]polycarbonate is dominated by the label at 150 ppm (Figure 2, bottom). DRAMA $\pi/2$ pulses produce a regular decrease in echo intensity with increasing evolution time (Figure 2, top) that is not observed for natural-abundance polycarbonate (data not shown).[18] The S/S_0 dephasing for the 150-ppm line is consistent with $^{13}C-^{13}C$ dipolar coupling for the carbonyl-carbon label of about 50 Hz.[13] A more quantitative estimate (and translation of the dipolar coupling into a distance) requires a model for chain packing, which will be discussed later.

CEDRA dephasing of the natural-abundance quaternary and methyl-carbon ^{13}C in [carbonyl-^{13}C]polycarbonate (Figure 3) and the homogeneous blend of labeled polycarbonates[7] (Figure 4) arises from coupling to carbonyl-carbon labels and is also qualitatively consistent with 50-Hz $^{13}C-^{13}C$ dipolar coupling. No significant dephasing is observed for the natural-abundance polycarbonate.[18] That is, $(S/S_0)_{\text{natural abundance}}$ is a constant close to 1. Neither carbonate nor isopropylidene groups undergo large amplitude motions in the glass at room temperature,[19,20] so sizable motional averaging of dipolar coupling can be ignored. The quaternary and methyl-carbon dephasing is complete after 50 ms (Figure 3, top right), indicating that all of these carbons are near carbonyl labels.

The DSR dephasing of the methyl-carbon signal in the blend is faster than the corresponding CEDRA dephasing. After 16 rotor cycles (13 ms), S/S_0 is about 0.85 in the CEDRA experiment (Figure 4) and 0.55 in

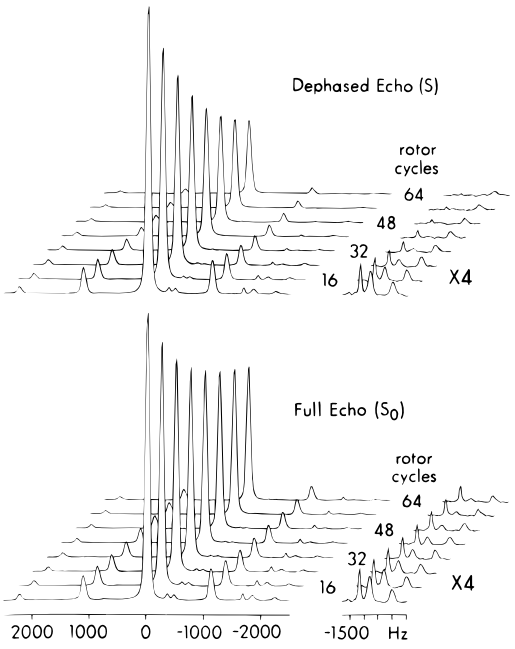

Figure 3. CEDRA dephased-echo (S) and full-echo (S_0) 15-MHz ^{13}C NMR spectra of [carbonyl-^{13}C]polycarbonate as a function of the number of rotor cycles of dephasing with magic-angle spinning at 1109 Hz. The CEDRA $n = 1$ condition is satisfied for the carbonyl-carbon peak and the average of the quaternary- and methyl-carbon peaks.

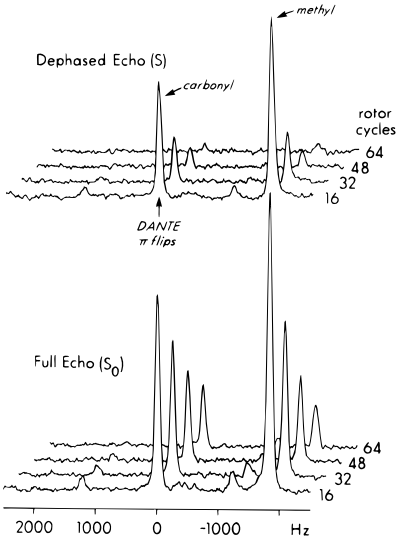

Figure 4. CEDRA dephased-echo (S) and full-echo (S_0) 15-MHz ^{13}C NMR spectra of a homogeneous blend of 95% [carbonyl-^{13}C]polycarbonate-d_{14} and 5% [methyl-^{13}C]polycarbonate as a function of the number of rotor cycles of dephasing with magic-angle spinning at 1222 Hz. The CEDRA $n = 1$ condition is satisfied for the carbonyl-carbon peak and the methyl-carbon peak. A 300−μs cross-polarization transfer discriminated against the carbonyl-carbon signal.

the DSR experiment (Figure 5). For polycarbonate, chemical-shift resolution depends on a distribution of isotropic shifts arising from variations in local packing. Thus, resolution at 15 MHz is similar to that at 75 MHz (compare Figures 2 and 3). Dipolar evolution experiments like CEDRA at a high magnetic field therefore have only a sensitivity advantage over those at a low magnetic field and have the disadvantage of more pulses for the same evolution time because the matching condition at high field demands a higher spinning speed.

Discussion

Interchain Dipolar Coupling and Local Orientational Order. The strong interchain dipolar coupling

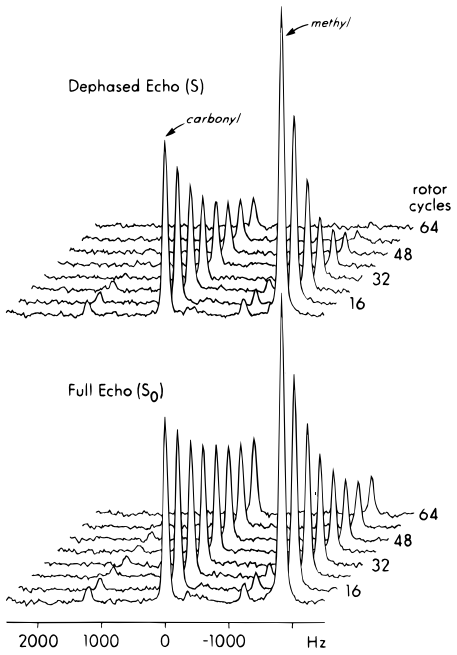

Figure 5. DANTE-selected homonuclear REDOR (DSR) dephased-echo (S) and full-echo (S_0) 15-MHz ^{13}C NMR spectra of a homogeneous blend of 95% [carbonyl-^{13}C]polycarbonate-d_{14} and 5% [methyl-^{13}C]polycarbonate as a function of the number of rotor cycles of dephasing with magic-angle spinning at 1222 Hz. The CEDRA $n = 1$ condition is satisfied for the carbonyl-carbon peak and the methyl-carbon peak. The DANTE-selective π pulse was on resonance for the carbonyl carbon. A 300−μs cross-polarization transfer discriminated against the carbonyl-carbon signal.

producing the dephasing of Figures 2−5 for polycarbonates in which all carbonyl carbons are ^{13}C labeled is only consistent with carbonate−carbonate and carbonate−isopropylidene proximity. This proximity is not the situation, for example, in the random packing model of Hutnik et al.[21] With random packing, there are simply too many sites with only long-range weak dipolar couplings to account for the experimental full dephasing. We therefore conclude that on a 10-Å scale the local orientational order of glassy polycarbonate is not completely random, and we suggest a model for the glass that has elements of crystalline-like packing.

We emphasize at the outset that our model will not be uniquely determined by the available NMR data. Nevertheless, some sort of model is needed to translate the experimental multicenter dephasing into interpretable distances. Naturally, we will demand that our model be consistent not only with the results of solid-state NMR distance experiments, but also with the results of X-ray and neutron scattering experiments, surface microscopy, and mechanical, thermal, and transport measurements. In addition, we will use the interchain distances obtained from the model as constraints on molecular dynamics simulations[22] which can account for experimentally determined phenylene ring-flip rates and activation energies. That is, we will insist that the model be consistent not only with all available structural results on polycarbonate, but with the results of chain-dynamics experiments as well. While our model will still not be uniquely determined, we will attempt to emphasize those features of the model which must be incorporated in any acceptable description of glassy polycarbonate.

Packing in a Crystal of Short Polycarbonate Chains. X-ray analysis of 4,4′-isopropylidenediphenyl-bis(phenyl carbonate), which we refer to as “dicarbon-

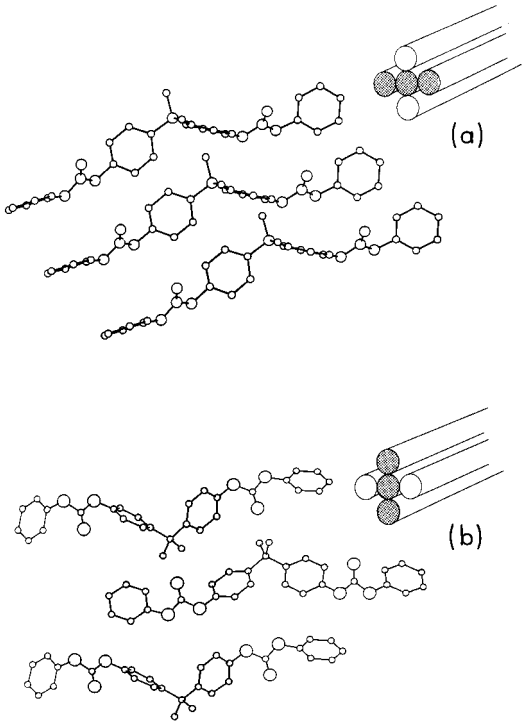

Figure 6. Parallel chain packing for polycarbonate based on the crystal structure of 4,4′-isopropylidenediphenylbis(phenyl carbonate). Each repeat unit is six-coordinate, with two flanking units from the same chain and four from nearest-neighbor chains (see inserts). A central chain is shown with its two in-register nearest neighbors (a) and its two out-of-register nearest neighbors (b). Conformation about the carbonate groups has been made all *trans* (that of the crystal structure is not) with in-register carbonate dipoles either parallel (panel a) or antiparallel (not shown). Intrachain neighboring phenyl rings are assumed orthogonal. Interchain neighboring phenyl rings are assumed to be either parallel (in-register chains) or orthogonal (out-of-register chains).

ate", reveals two kinds of nearest neighbors for an individual dicarbonate chain: those in register and those shifted out of register.[11] Because the dicarbonate chains are short, tight packing in the crystal is possible despite conformational arrangements about the two carbonate groups, leading to pronounced bowing. (In fact, some next-nearest-neighbor dicarbonate distances are comparable to the nearest-neighbor distances because of the bowing of the individual molecules.) Long polycarbonate chains can pack tightly only if just a few bowing arrangements are present. Mostly, polycarbonates will tend to form chains whose carbonate linkages are in a slightly distorted trans conformation,[21,23,24] resulting in bundles of locally parallel chains. This sort of parallel-chain packing is illustrated for dicarbonate in Figure 6. Relative to any single dicarbonate as a reference, the in-register dicarbonate neighbors have carbonyl and quaternary carbons in the same plane as the quaternary and carbonyl carbons of the reference chain (Figure 6a), whereas the out-of-register dicarbonate neighbors have quaternary and carbonyl carbons in planes above or below the reference plane (Figure 6b). The minimum intermolecular distance between two carbonyl carbons of in-register dicarbonates is 6.6 Å compared to 6.1 Å for out-of-register dicarbonates, while the corresponding carbonyl to nearest methyl-carbon distance is 5.4 Å in register and 4.5 Å out of register.

We adopt a model for locally parallel chain segments in polycarbonate based on Figure 6. Each chain in the model has two nearest-neighbor chains in register and two out of register. Any given monomer unit is therefore approximately six-coordinate, with two surrounding

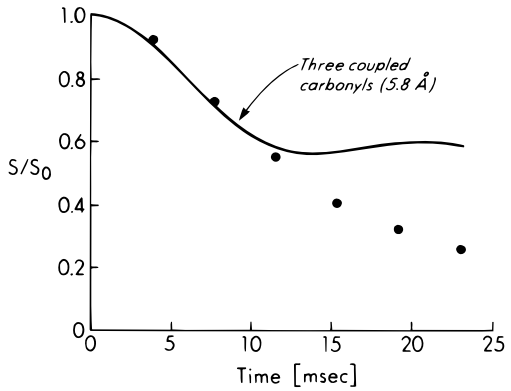

Figure 7. Experimental DRAMA dephasing for [carbonyl-^{13}C]polycarbonate. The solid circles show $(S/S_0)_{\text{label}}/(S/S_0)_{\text{natural abundance}}$, where $(S/S_0)_{\text{label}}$ is from Figure 2. The data for $(S/S_0)_{\text{natural abundance}}$ are not shown (see ref 18). The solid line was calculated by using the packing model of Figure 6 and assuming that each carbonyl carbon has two equivalent nearest neighbors at 5.8 Å.

monomer units from the same chain, two from in-register chains, and two from out-of-register chains. The in-register chains can have their carbonate groups either parallel (Figure 6a) or antiparallel (not shown). Packing of the parallel carbonates is tighter. The out-of-register chains pack around a central chain so that there is only one short, nearest-neighbor distance between the carbonate and isopropylidene groups (Figure 6b). Nearest-neighbor rings are shown orthogonal to one another,[11,21] both within a chain and from chain to chain, although this is not an essential feature of the packing because the rings are known to be mobile.[19] That is, the rings undergo rapid, continuous oscillations about their C_2 axes as well as flips. Thus, there is no static orthogonal ring orientation. In addition, molecular dynamics simulations have shown recently that if the orthogonality of rings is imposed as a time-averaged initial condition, this arrangement does not persist.[22] The packing of all-trans chains shown in Figure 6 is similar to that proposed by Bonart for crystalline polycarbonate.[24]

Interpretation of DRAMA and CEDRA Dephasing. Using the model illustrated in Figure 6, we see that each polycarbonate carbonyl carbon has two (in-register) ^{13}C-labeled carbonate nearest neighbors. This arrangement of coupled homonuclear spins in a linear array[25] means that for a given internuclear separation, the magnetization from half of the labeled carbonyl carbons dephases twice as fast as expected on the basis of a single nearest neighbor, and that from the other half does not dephase at all (Figure 7, solid line). Using only the reliable *initial* DRAMA dephasing[15] to define the carbon−carbon interaction, we estimate the carbonyl−carbonyl dipolar coupling as 80 Hz, corresponding to a ^{13}C−^{13}C distance of 5.8 Å, comparable to the corresponding distance in crystalline dicarbonate. More distant neighbors are undoubtedly responsible for the dephasing after 10 ms, but we make no attempt to account for this dephasing quantitatively.

Each quaternary carbon has a single, nearest-neighbor carbonyl carbon (Figures 6 and 8) which dominates CEDRA dephasing. The placements of carbonyl carbons shown in Figure 8 were taken from the dicarbonate crystal stucture, as modified by the all-*trans* conformational requirement. We realize that in the glass the exact details of this array are not relevant. Variations in spacings produce packing irregularities that can only be described statistically using a distribution function. Nevertheless, we will retain as appropri-

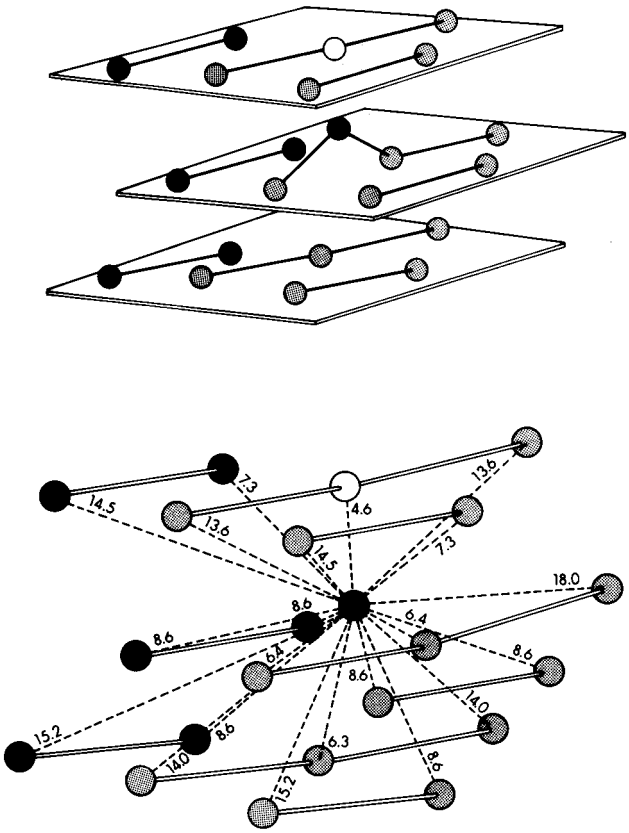

Figure 8. Model for polycarbonate packing (top), showing both in-register neighbors within a central plane and out-of-register neighbors in planes above and below. Carbonyl carbons of all but one of the carbonate moieties are connected by virtual bonds (straight lines). One chain in each plane has been lengthened. A single quaternary carbon of the central chain is shown (solid circle). This quaternary carbon has only one nearest-neighbor, out-of-register carbonyl carbon (open circle), with the other out-of-register carbonyl carbons, and both in-register and in-chain carbonyl carbons, significantly farther away (bottom). Distances are inferred from the crystal structure of 4,4′-isopropylidenediphenylbis(phenyl carbonate).

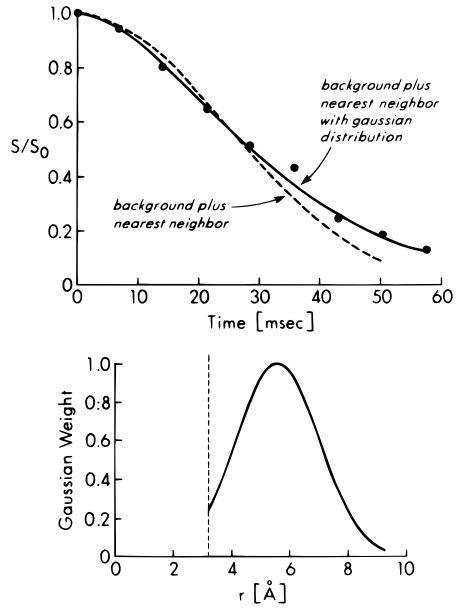

Figure 9. Experimental CEDRA dephasing for the quaternary carbon of [carbonyl-^{13}C]polycarbonate. The solid circles show $(S/S_0)_{\text{label}}/(S/S_0)_{\text{natural abundance}}$, where $(S/S_0)_{\text{label}}$ is from Figure 3. The data for $(S/S_0)_{\text{natural abundance}}$ are not shown (see ref 18). The solid line was calculated using the packing model of Figure 6 and a modified version of the internuclear distances of Figure 8 (bottom). The modifications were (i) a lengthening of the nearest-neighbor quaternary-carbon to carbonyl-carbon distance from 4.6 to 5.6 Å, (ii) a distribution of the nearest-neighbor distance as shown in the bottom panel, and (iii) an increase in all non-nearest-neighbor quaternary-carbon to carbonyl-carbon distances of 7%.

ate for our model of the glass, the notions of (i) approximate six-coordinate repeat-unit packing and (ii) a single nearest-neighbor chain.

The background dephasing of the quaternary-carbon magnetization due to the collection of next-nearest neighbor carbonyl ^{13}C labels (Figure 9) can be calculated directly by assuming that the carbonyl spins are not coupled to each other. This condition is satisfied because fast magic-angle spinning suppresses the weak homonuclear coupling between carbonyl carbons and the single π pulse per rotor period induces no dephasing for homonuclear coupling between spins with no isotropic chemical-shift separation. In addition, under CEDRA spinning conditions, homonuclear flip-flops between quaternary- and carbonyl-carbon spins are suppressed and this ensures the independence of the couplings between those carbons.[16] Thus, the powder average of a sum of independent dephasings (resulting from the coupling between one quaternary carbon and a collection of carbonyl carbons) equals the powder average of the product of those dephasings: $S/S_0 = \langle\cos(\sum_i \phi_{Di})\rangle_{\text{space and spin}} = \langle\prod_i \cos(\phi_{Di})\rangle_{\text{space}}$, where ϕ_{Di} is the phase accumulation[1] resulting from the homonuclear dipolar coupling between a quaternary carbon and the i*th* carbonyl carbon, the first angle bracket indicates an average over space and spin coordinates, and the second angle bracket indicates just a spatial powder average. The average over spin coordinates includes dephasing by ^{13}C−^{13}C pairs that have parallel spins (positive ϕ_D) and anti-parallel spins (negative ϕ_D) and takes advantage of the additivity of arguments for the products of exponentials.[26] This is a standard averaging procedure in SEDOR calculations for multiple dephasing spins.[27]

Using Figure 8 to establish the positions of the carbonyls relative to a specific quaternary carbon, the powder average is not complicated to perform. We have found that the next-nearest neighbors account for only about 50% of the observed dephasing even after 50 ms (not shown). Because there are so many next-nearest neighbors, minor variations in their positions have little effect on the calculated quaternary-carbon dephasing. Thus, the fact that the next-nearest-neighbor positions are not known accurately is not critical. Addition of the single nearest-neighbor coupling to the dephasing calculation is still not sufficient to account for the experimentally observed dephasing. This calculation produces too little dephasing for short evolution times and too much dephasing for long evolution times (Figure 9, dotted line). Thus, increasing or decreasing the nearest-neighbor distance cannot improve the match of calculated to experimental dephasing in both regimes. However, a *distribution* which places about 90% of the quaternary-carbonyl ^{13}C−^{13}C distances within ±20% of a 5.6-Å average (Figure 9, bottom panel) results in satisfactory agreement between experiment and calculation (Figure 9, solid line). The need for this distribution emphasizes that interchain spacings within a bundle, and from bundle to bundle, do not have the regularity of a crystal. No distribution of distances is required to match the observed CEDRA dephasing of the methyl-carbon magnetization (Figure 10, solid line), presumably because of the averaging over two different methyl-carbon positions. In the blend of ^{13}C-carbonyl and methyl-^{13}C polycarbonates, labeled methyl carbons have no in-chain labeled carbonyl neighbors. Removal of the two close, next-nearest-neighbor carbonyls (see

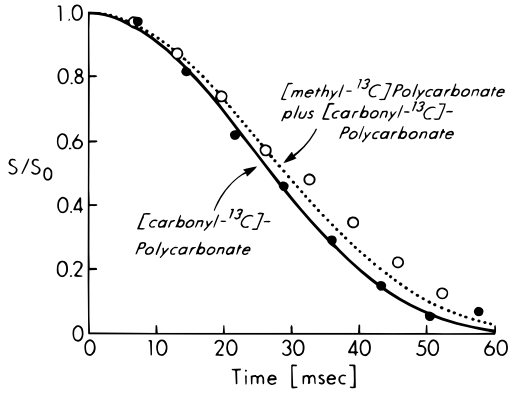

Figure 10. Experimental CEDRA dephasing for the methyl carbon of [carbonyl-^{13}C]polycarbonate, and for the methyl carbon of a homogeneous blend of 95% [carbonyl-^{13}C]polycarbonate-d_{14} and 5% [methyl-^{13}C]polycarbonate. The solid circles show $(S/S_0)_{\text{label}}/(S/S_0)_{\text{natural abundance}}$, where $(S/S_0)_{\text{label}}$ is from the [carbonyl-^{13}C]polycarbonate results of Figure 3. The data for $(S/S_0)_{\text{natural abundance}}$ are not shown (see ref 18). The open circles show the corresponding scaled dephasing for the blend of Figure 4. The solid line was calculated as described in the caption to Figure 9 by assuming that the average methyl-carbon to nearest-neighbor carbonyl-carbon distance was 5.0 Å and was not distributed. A separate S/S_0 was calculated for each methyl carbon of the isopropylidene group, and the results were averaged. The dotted line was calculated in the same way as the solid line except that the dephasing contributions from the in-chain carbonyl carbons at 6.4, 6.4, and 18.0 Å, respectively, were removed from the background. (See Figure 8.)

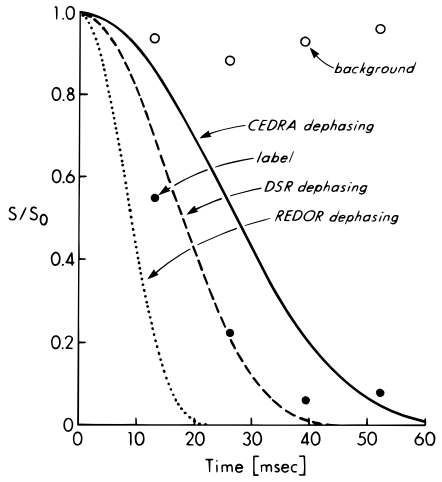

Figure 11. Experimental DANTE-selected homonuclear REDOR (DSR) dephasing for the methyl carbon of a homogeneous blend of 95% [carbonyl-^{13}C]polycarbonate-d_{14} and 5% [methyl-^{13}C]polycarbonate from Figure 5 (closed circles) and for the methyl carbon of natural-abundance polycarbonate (open circles). The solid line was calculated as described in the caption to Figure 10 for CEDRA dephasing and is presented as a reference. The dotted line was calculated by assuming δ-function REDOR dephasing pulses acting only on the carbonyl carbon, and the dashed line was calculated by assuming that the long DANTE π pulses are half as effective as the δ-function pulses.

Figure 8, bottom) reduces the methyl-carbon CEDRA dephasing by about 10% (Figure 10, open circles), consistent with expectations based on the packing model (Figure 10, dotted line).

Homonuclear REDOR. For the CEDRA $n = 1$ condition, dephasing is one-third of that produced by a comparable REDOR experiment using hypothetical selective δ-function pulses.[2] The observed DSR dephasing is between this REDOR limit and CEDRA dephasing (Figure 11), suggesting that the long, selective DANTE pulses affect dipolar evolution for only a fraction of a rotor cycle. A quantitative description of the DSR experiment is not yet available. Nevertheless, the qualitative agreement between CEDRA and DSR dephasing results is only consistent with strong interchain ^{13}C-^{13}C dipolar coupling and short interchain distances, and therefore supports a tight chain-packing model for polycarbonate.

Model-Independent Description of Packing. We emphasize that the structures shown in Figures 6 and 8 are illustrations of a model, not a uniquely determined structure. Features of the actual structure of polycarbonate may differ significantly. Nevertheless, those details of our model established experimentally by NMR must be present in any realistic description of polycarbonate. The most important of these include tight packing, local orientational order, a distribution of interchain spacings, and a carbonyl-carbon to quaternary-carbon, nearest-neighbor interchain distance of about 6 Å for each repeat unit.

Bundle Model. The model illustrated in Figure 6 corresponds to one domain in the glass. Because a polycarbonate glass has no long-range order, local variations in packing, associated with conformational variations about the carbonate and phenyl groups, necessarily must occur.[6] Thus, the direction of local parallelism of the bundle at such sites will abruptly change, thereby defining a new bundle and a different collection of locally parallel chains.

A single polycarbonate chain can weave between bundles so that the mean end-to-end distance of the chain has its unperturbed dimension. Even though our NMR measurements are restricted to a 10-Å scale, we envision that each bundle consists of three or four repeat units of a collection of five to ten locally parallel chains forming a domain of the order of 50 Å. A significantly smaller average domain size would involve so many cis−trans conformational defect sites that the tight chain packing demanded by the dipolar-coupling results of Figures 2−5 could not be met because of the pronounced bowing of individual chains. Because each chain must be associated with its single nearest-neighbor chain (Figure 6) to account for the DRAMA, CEDRA, and DSR dephasing (Figures 9−11), even the peripheral members of a bundle will experience packing interactions comparable to those in the interior. These packing interactions are distributed (the variation in nearest-neighbor chain distance is ±20%; see distribution of Figure 9, bottom panel), so there are no density variations correlated with bundle domains that could be detected by either X-ray[28,29] or neutron scattering,[30] and none have been observed. However, the presence in amorphous polycarbonate of roughly parallel short sequences with an average intersegmental distance of about 5 Å has been inferred from neutron scattering.[31]

Variations in local interchain spacings will affect chain dynamics that depend both on packing within the bundle and on packing between bundles. The resulting wide-range dynamic heterogeneity implied by the model of Figure 6 (modified by the distribution of Figure 9) is consistent with the results of mechanical,[32] thermal,[32] diffusivity,[33,34] and NMR relaxation measurements.[9,19,32,35,36] In addition, the model suggests that surface irregularities associated with the local orientational order of bundles are present, and these have been visualized recently by noncontact atomic force microscopy.[37]

The three homonuclear carbon−carbon interchain distances obtained from the analyses represented by Figures 7, 9, and 10 have been used recently as

constraints on energy-minimized molecular dynamics simulations, the results of which support the essential features of the model of Figure 6. These simulations successfully show ring flips and correctly predict (i) ring-flip activation energies for polycarbonate, (ii) the three heteronuclear carbon−deuterium interchain distances from REDOR measurements, and (iii) the experimental bulk density (see companion paper in this Journal by Whitney and Yaris[22]).

Acknowledgment. The [carbonyl-^{13}C]polycarbonate was the generous gift of J. Michael Hewitt (Eastman Kodak Co., Rochester, NY). The authors thank Jinhuang Wu and Professor Albert F. Yee (University of Michigan) for preparation of the [methyl-^{13}C]polycarbonate. The [carbonyl-^{13}C]polycarbonate-d_{14} was also prepared by Jinhuang Wu as described in ref 34. This work was supported by NSF grant DMR-9015864.

References and Notes

(1) Gullion, T.; Schaefer, J. *Adv. Magn. Reson.* **1989**, *13*, 57.
(2) Gullion, T.; Vega, S. *Chem. Phys. Lett.* **1992**, *194*, 423.
(3) Tycko, R.; Daggagh, G. *Chem. Phys. Lett.* **1990**, *173*, 461.
(4) Raleigh, D. P.; Levit, M. H.; Griffin, R. G. *Chem. Phys. Lett.* **1988**, *146*, 71.
(5) Romiszowski, P.; Yaris, R. *J. Chem. Phys.* **1991**, *95*, 6738.
(6) Hutnik, M.; Argon, A. S.; Suter, A. W. *Macromolecules* **1991**, *24*, 5970.
(7) Schmidt, A.; Kowalewski, T.; Schaefer, J. *Macromolecules* **1993**, *26*, 1729.
(8) Lee, P. L.; Schaefer, J. *Macromolecules* **1995**, *28*, 1921.
(9) Schaefer, J.; Stejskal, E. O.; Perchak, D.; Skolnick, J.; Yaris, R. *Macromolecules* **1985**, *18*, 368.
(10) Jho, J. Y.; Yee, A. F. *Macromolecules* **1991**, *24*, 1905.
(11) Perez, S.; Scaringe, R. P. *Macromolecules* **1987**, *20*, 68.
(12) Henrichs, P. M.; Luss, H. R. *Macromolecules* **1988**, *21*, 2731.
(13) Tycko, R.; Smith, S. O. *J. Chem. Phys.* **1993**, *98*, 932.
(14) Gullion, T.; Baker, D.; Conradi, M. S. *J. Magn. Reson.* **1990**, *89*, 479.
(15) Klug, C. A.; Zhu, W.; Merritt, M. E.; Schaefer, J. *J. Magn. Reson. A* **1994**, *109*, 134.
(16) Zhu, W.; Klug, C. A.; Schaefer, J. *J. Magn. Reson. A* **1994**, *108*, 121.
(17) Holl, S. M.; McKay, R. A.; Gullion, T.; Schaefer, J. *J. Magn. Reson.* **1990**, *89*, 620.
(18) Zhu, W. Thesis, Washington University, 1994.
(19) Schaefer, J.; Stejskal, E. O.; McKay, R. A.; Dixon, W. T. *Macromolecules* **1984**, *17*, 1479.
(20) Poliks, M. D.; Gullion, T.; Schaefer, J. *Macromolecules* **1990**, *23*, 2678.
(21) Hutnik, M.; Gentile, F. T.; Ludovice, P. J.; Suter, U. W. *Macromolecules* **1991**, *24*, 5962.
(22) Whitney, D. R.; Yaris, R. *Macromolecules* **1997**, *30*, 1741.
(23) Jones, A. A. *Macromolecules* **1985**, *18*, 902.
(24) Bonart, A. *Makromol. Chem.* **1966**, *92*, 149.
(25) Cho, G.; Yesinowski, J. P. *Chem. Phys. Lett.* **1993**, *205*, 1.
(26) Boyce, J. B. Thesis, University of Illinois, Urbana-Champaign, 1972, p 28.
(27) Wang, P. K.; Slichter, C. P.; Sinfelt, J. H. *Phys. Rev. Lett.* **1984**, *53*, 82.
(28) Lin, W.; Kramer, E. J. *J. Appl. Phys.* **1973**, *10*, 4288.
(29) Renninger, A. L.; Wicks, G. G.; Uhlmann, D. R. *J. Polym. Sci. Phys.* **1975**, *13*, 1247.
(30) Cervinka, L.; Fischer, E. W.; Dettenmaier, M. *Polymer* **1991**, *32*, 12.
(31) Cervinka, L.; Fischer, E. W.; Hahn, K.; Jiang, B.-Z.; Hellman, G. P.; Kuhn, K.-J. *Polymer* **1987** *28*, 1287.
(32) Lee, P. L.; Kowalewski, T.; Poliks, M. D.; Schaefer, J. *Macromolecules* **1995**, *28*, 2476.
(33) Lee, P. L.; Schaefer, J. *Macromolecules* **1992**, *25*, 5559.
(34) Lee, P. L.; Xiao, C.; Wu, J.; Yee, A. F.; Schaefer, J. *Macromolecules* **1995**, *28*, 6477.
(35) Spiess, H. W. *Colloid Polym. Sci.* **1983**, *261*, 193.
(36) O'Gara, J. F.; Jones, A. A.; Hung, C.-C.; Inglefield, P. T. *Macromolecules* **1985**, *18*, 1117.
(37) Kowlaweski, T.; Schaefer, J. *Polym. Mater. Sci. Eng.* **1997**, *76*.

MA961144U